reactions

MDPI

Review

Incorporation of Spin Labels and Paramagnetic Tags for Magnetic Resonance Studies Using Cycloaddition Reactions as a Tool

Amarendra Nath Maity [1], Amiya Kumar Medda [2] and Shyue-Chu Ke [1,*]

[1] Department of Physics, National Dong Hwa University, Hualien 97401, Taiwan; maity@gms.ndhu.edu.tw
[2] Department of Chemistry, Indian Institute of Technology Kanpur, Kanpur 208016, U.P., India; amiya@iitk.ac.in
* Correspondence: ke@gms.ndhu.edu.tw

Abstract

The cycloaddition reaction is one of the most common reactions in organic chemistry. It has been applied in various fields. Herein, we focus on the application of cycloaddition reactions in investigating biological molecules and materials using magnetic resonance techniques. To facilitate magnetic resonance studies such as electron paramagnetic resonance (EPR) spectroscopy and paramagnetic nuclear magnetic resonance (NMR) spectroscopy, there is often a requirement to attach spin labels and paramagnetic tags to the system of interest. The cycloaddition reaction is one of the ways to tether these spin labels and paramagnetic tags. In this review, we highlight the applications of various cycloaddition reactions such as the Cu(I)-catalyzed azide–alkyne cycloaddition (CuAAC) reaction, the strain-promoted azide–alkyne cycloaddition (SPAAC) reaction and the Diels–Alder reaction in the interdisciplinary field of magnetic resonance studies of biomolecules, including proteins, nucleic acids, carbohydrates, lipids and glycans, as well as materials.

Keywords: cycloaddition reaction; spin label; paramagnetic tag; azide–alkyne cycloaddition; click chemistry

1. Introduction

In synthetic organic chemistry, the cycloaddition reaction is one of the most favored tools to get easy access to cyclic compounds [1–9]. The applications of cycloaddition reactions transcend various fields of chemistry and biology. In this review, we showcase the application of cycloaddition reactions towards magnetic resonance studies of biological molecules and materials. The purpose of this review is to underscore the interplay among the apparently independent fields—cycloaddition reactions and magnetic resonance studies of biomolecules and materials. This review article intends to present a comprehensive survey of the cycloaddition reactions that are employed to attach spin labels and paramagnetic tags to biomolecules and materials to facilitate the magnetic resonance studies on them. Given the interdisciplinary nature of the topic, we briefly introduce the key topics at the beginning of the review, spanning three sections. In the first section, we provide a superficial view of each topic, emphasizing the terms that we come across in this review. We cite relevant review articles and book chapters that can be used to gain a deep understanding of the respective topics. In the second section, we discuss the azide–alkyne cycloaddition (AAC) reaction—emphasizing the Cu(I)-catalyzed azide–alkyne cycloaddition (CuAAC) reaction and the strain-promoted azide–alkyne cycloaddition (SPAAC) reaction—and the

Check for updates

Academic Editors: Donatella Giomi and Fabrizio Machetti

Received: 29 December 2025
Revised: 30 January 2026
Accepted: 1 February 2026
Published: 6 February 2026

Copyright: © 2026 by the authors. Licensee MDPI, Basel, Switzerland. This article is an open access article distributed under the terms and conditions of the Creative Commons Attribution (CC BY) license.

Diels–Alder reaction, which are frequently employed to stich spin labels and paramagnetic tags. In the third section, the use of electron paramagnetic resonance (EPR) and paramagnetic nuclear magnetic resonance (NMR) spectroscopies to study biomolecules is presented. In the following section, the features of spin labels and paramagnetic tags are elaborated upon. In the fourth section, we summarize the applications of cycloaddition reactions such as CuAAC, SPAAC, and the Diels–Alder reactions to tailor biomolecules such that they are ready for EPR and paramagnetic NMR studies. We note that, in the schemes throughout this article, the moieties involving the cycloaddition reactions are highlighted with orange color, while the spin label and paramagnetic tag moieties are highlighted with light blue color. Finally, conclusions and an outlook are provided.

2. Cycloaddition Reactions

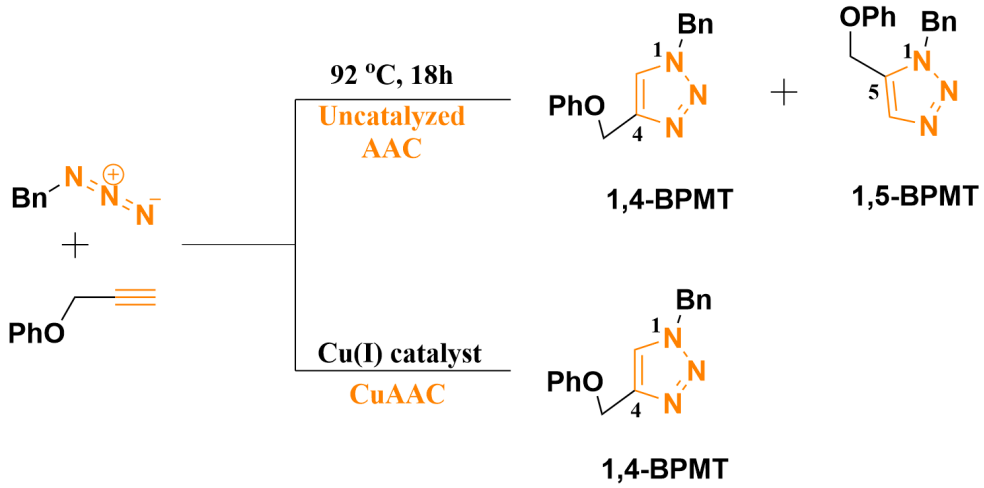
Cycloaddition reactions are a class of organic reactions that are very useful in synthetic organic chemistry. Definition, classification, and applications of cycloaddition reactions have been elaborated upon in detail in the literature [10,11]. The AAC reaction and the Diels–Alder reaction belong to the class of cycloaddition reactions. These reactions have been leveraged for tethering the spin labels and paramagnetic tags to biological systems as well as materials.

2.1. Azide–Alkyne Cycloaddition (AAC) Reactions

The typical azide–alkyne coupling reaction (AAC), as illustrated below in Scheme 1, refers to the cycloaddition reaction between an azide unit and an alkyne unit [12]. The traditional uncatalyzed AAC reaction was investigated in depth and is referred to as the 1,3-dipolar cycloaddition by Huisgen [13–15]. This reaction pathway affords both 1-benzyl-4-(phenoxymethyl)-1*H*-1,2,3-triazole (1,4-BPMT) and 1-Benzyl-5-phenoxymethyl-1*H*-[1,2,3]triazole (1,5-BPMT) isomers in almost a 1:1.6 ratio at around 92 °C [16]. In the first decade of this century, a more benign method of AAC reaction using Cu(I) as the catalyst was initiated and developed independently by Sharpless [16] and Meldal [17]. This Cu(I)-catalyzed azide–alkyne cycloaddition reaction, known as the CuAAC reaction, is the most renowned representative of "click chemistry". Click chemistry—the concept of simple and straightforward organic transformations with high yield that are specific, quick, and reliable— was coined by Sharpless in 2001 [18]. In the case of the CuAAC reaction, it has been reported that it is a 10^7 times faster reaction than the AAC reaction [19]. Of particular interest, as far as the CuAAC reaction is concerned, is the circumvention of the need for higher temperatures. This feature makes the CuAAC reaction one of the most lucrative options for application in biological samples, which are typically not heat-tolerant. Another notable feature of CuAAC is that it is a regioselective reaction (only 1,4-BPMT as the product with a yield of 91%) [16]. Contrary to the above observation, Abu-Orabi and coworkers reported an uncatalyzed [3+2] cycloaddition between aryl azide and ethyl propiolate, affording a fully regioselective 1,4-disubstituted 1,2,3-triazole product [20,21].

Subsequently, Bertozzi took this concept to another level by applying click reactions in vivo [22]. For applications of bioorthogonal chemistry in living systems by circumventing the biocompatibility issue associated with Cu (I), Bertozzi and coworkers developed "Cu-free click chemistry", in which, in the absence of a Cu(I) catalyst, a strained-cyclooctyne moiety, by playing the role of an alkyne component, facilitates the AAC reaction; it is referred to as the strain-promoted azide–alkyne cycloaddition (SPAAC) reaction [22,23]. Subsequently, SPAAC was applied to label biomolecules such as proteins [24], nucleotides [25], carbohydrates [26], and lipids [27]. The contributions to these interdisciplinary fields were recognized by awarding the Nobel Prize in Chemistry to Professors K. Barry Sharpless, Morten Meldal, and Carolyn R. Bertozzi in 2022 [28]. Recently, Bauer and coworkers

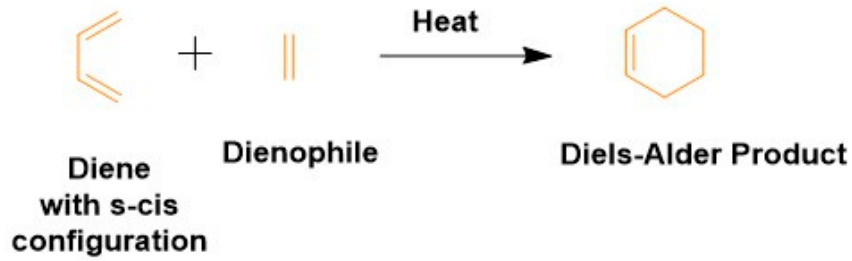
showcased the recent applications of click chemistry in radiopharmaceutical chemistry in an excellent review article [29].



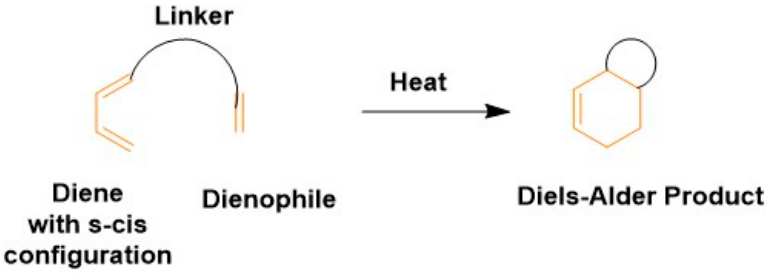
Scheme 1. Uncatalyzed and Cu(I)-catalyzed AAC reactions.

2.2. Diels–Alder Reaction

The Diels–Alder reaction, an important type of C–C bond-forming organic reaction under the class of cycloaddition reaction, was discovered by Otto Diels and Kurt Alder, who won the Nobel prize in 1950 for their remarkable work [30]. A diene (electron-rich and can be either acyclic or cyclic) and a dienophile (electron-deficient) are combined together to form a six-membered cyclic compound in which three π bonds break, and two new σ bonds form along with one π bond (Scheme 2). The stereochemical aspect was successfully depicted as retaining the configuration with respect to the reactants [31], whereas, in a recently studied example, it was lost [32]. Moreover, diradical and zwitterionic intermediate proposals have been put forward and evaluated with the help of a computational study [33]. These facts dictate changes in the mechanistic pathway, which are governed by the nature of the substituents present in the diene and dienophile, thereby controlling the reactivity of the system. Using advanced computational techniques, such as molecular electron density theory (MEDT), Domingo and coworkers revisited the mechanistic pathways for this reaction, providing deeper insights into the Diels–Alder reaction mechanism [34,35]. The intra-molecular Diels–Alder reaction is depicted in Scheme 3, where diene and dienophile are present in the same molecule, and normally there should be a three-carbon distance between them.



Scheme 2. Inter-molecular Diels–Alder reaction.



Scheme 3. Intra-molecular Diels–Alder reaction.

The functionalization of graphene and graphite employing the Diels–Alder reactions has been investigated both experimentally and computationally [36–40].

3. Magnetic Resonance Studies

NMR spectroscopy is the most widely known magnetic resonance technique that is employed to study the structure and properties of molecules and materials. Nevertheless, the presence of a paramagnetic center in the sample creates complications in the NMR spectra by broadening the resonance signals, and it is little wonder. EPR spectroscopy was simultaneously developed to study the paramagnetic samples. On the other hand, paramagnetic NMR has been developed to study samples containing paramagnetic centers by converting drawbacks into advantages.

3.1. Electron Paramagnetic Resonance (EPR)

EPR spectroscopy is one of the best analytical techniques to study paramagnetic samples. EPR spectroscopy detects the unpaired electron spins and provides geometric and electronic environmental information around the locus of the paramagnetic center. The theory and applications of EPR have been explored in numerous books [41–45]. The applications of EPR in various biological systems have been documented in many books and review articles; of particular interest, a book chapter on the EPR of metalloproteins was written by Palmer [46], a special edition of the *Chemical Review* on radical enzymes was edited by Banerjee [47], and book chapters on the EPR of B_{12}-dependent enzymes were written by Pilbrow [48] and Gerfen [49]. Continuous wave EPR spectroscopy that operates at the X-band (9.8 GHz) is the most common EPR technique. Recently, high-frequency EPR methods have also been increasingly used to understand the paramagnetic systems. Moreover, advanced EPR techniques such as double-electron electron resonance (DEER), also known as pulsed electron double resonance (PELDOR), electron nuclear double resonance (ENDOR), electron spin echo envelope modulation (ESEEM), and hyperfine sublevel correlation (HYSCORE) have been routinely used to investigate complex systems [50]. The parameters obtained from EPR lineshape analysis provide information about the motions of the spin label. These parameters can be correlated with protein conformation and dynamics [51]. Spin–lattice (longitudinal) and spin–spin (transverse) relaxation processes modulate the EPR lineshapes. The implications of spin–spin relaxation time in distance measurements by pulsed EPR were discussed by Jeschke and coworkers [52,53], while the dependence of spin–lattice relaxation on molecular motions was portrayed by Eaton and Eaton [54]. DEER spectroscopy has been proven to be an excellent tool to investigate protein dynamics, especially in membrane proteins, by estimating long-range distances between the two paramagnetic centers [55–58].

3.2. Paramagnetic NMR

Sacconi and coworkers, who used the paramagnetic NMR technique to analyze Ni(II) complexes with Schiff bases in solution, published their work for the first time in two

consecutive articles in 1966 [59,60]. Since then, various research groups have been actively working in this area to convert the inherent disadvantages—the line broadening, fast relaxation, and hyperfine interactions—into a fruitful manner for understanding the structure and chemistry of paramagnetic organometallic complexes and proteins, and to extract the useful information about dynamics in solution in terms of time scale [61,62]. Paramagnetic centers exert various effects on the NMR spectra. The major paramagnetic parameters include (1) the shift in resonances of the NMR-active nuclei, called hyperfine shifts, which are composed of two parameters—pseudocontact shifts (PCSs) and Fermi-contact shifts; (2) paramagnetic relaxation enhancements (PREs); and (3) paramagnetic residual dipolar couplings (pRDCs). In the context of protein structural determinations, these paramagnetic parameters are referred to as paramagnetic restraints. Ravera and coworkers elaborated on how these paramagnetic restraints allow the refinement of protein structures [63]. The role played by paramagnetic NMR in gaining insights into the structure and dynamics of membrane proteins was recorded in several published works [55,64,65].

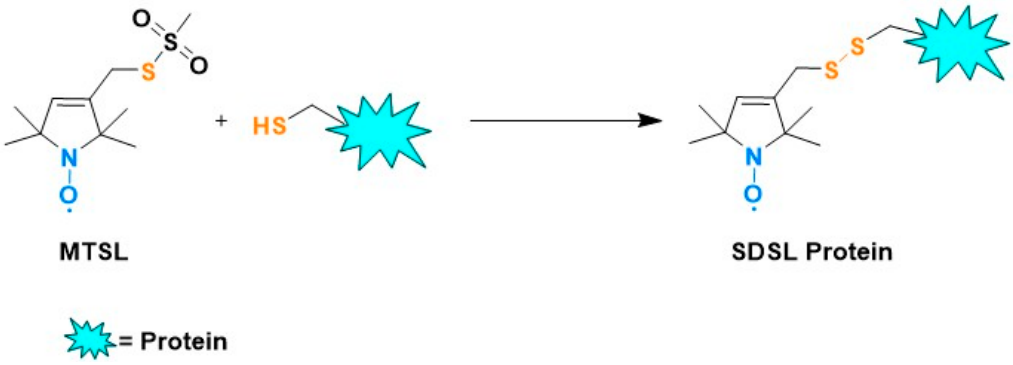
4. Spin Labels and Paramagnetic Tags

EPR and paramagnetic NMR have been used to extract information from systems containing a paramagnetic center. The dynamics of biomolecules can be uncovered using EPR experiments by measuring the distance between two paramagnetic centers present in the system. For example, in the case of vitamin B12-dependent enzymes, many mechanistic insights, including the evidence for the requirement of large-scale conformational movements during the catalysis, were obtained from EPR and ESEEM experiments by measuring the distance between the two paramagnetic centers [47,66–76]. Similarly, paramagnetic NMR has emerged as a powerful tool for studying metalloproteins [63,77–79]. It provides valuable data to enhance structural resolution as well as to investigate protein dynamics. Nevertheless, the presence of paramagnetic centers in biological systems is rather scarce, thus making EPR and paramagnetic NMR redundant in the vast cases of biomolecules. To circumvent this, the concept of introducing foreign paramagnetic centers into the diamagnetic systems was mooted. Spin labels and paramagnetic tags refer to molecules that have unpaired electrons, which can be attached to macromolecules to introduce paramagnetic effects. The term spin label is commonly used in the realm of EPR studies, while the term paramagnetic tag is used in the field of NMR studies. Sometimes, there were instances of cross-domain references. Nonetheless, throughout this review, we follow the convention mentioned above.

4.1. Spin Labels

The term spin labels stems from the purpose these molecules serve. These molecules are employed to label a system of interest with an unpaired electron spin. Site-directed spin labeling (SDSL) for EPR refers to the technique in which a spin probe is attached to a specific site on a biomolecule. SDSL was first developed for proteins and later extended to other systems. Traditionally, a free cysteine residue of a protein is identified and chemically linked to the spin probe. A nitroxide radical serves the purpose of the spin probe. Methanethiosulfonate nitroxide radical spin label (MTSL) reacts with the sulfhydryl group of the cysteine side chain by forming a disulfide bond to graft the nitroxide spin label onto the protein (Scheme 4) [57]. Later, the SDSL technique was extended beyond disulfide coupling. Another way to introduce spin labels to the protein is the genetic encoding of noncanonical amino acids (ncAAs) [80]. Genetically encoded nitroxide amino acids were used as spin labels for distance measurements by EPR spectroscopy [81]. Paredes and coworkers reported a rapid method to label RNA using CuAAC [82]. SDSL EPR studies of nucleic acids were documented in a book chapter by Shelke and Sigurdsson [83]. The utility

of the toolkit comprising SDSL and EPR spectroscopy for exploring protein backbone dynamics was highlighted in the review articles by Columbus and Hubbell [84], while Roser and coworkers summarized its applications to protein distance determinations in cells [85]. Early advances in the employment of SDSL in conjunction with DEER spectroscopy were tracked by Fanucci and Cafiso [51].



Scheme 4. Attachment of MTSL to the protein.

4.2. Paramagnetic Tags

Metal ions containing unpaired electrons are capable of exerting paramagnetic effects, thereby making them the automatic choices to be part of the paramagnetic tags. Metal ions belonging to the 3d block and the 4f block are of particular interest. Mn(II), Co(II), and Fe(III) of the 3d block have been studied thoroughly, while the Gd(III) ion of the 4f block has exceptional properties to act as a paramagnetic tag. Gd(III) ion possesses a strong isotropic magnetic susceptibility and produces exceptionally strong PREs. Thus, the most popular choice of the paramagnetic tag is a Gd(III) ion coordinated with organic ligands. Fe(II) tags coordinated to various [2,2′:6′,2″-terpyridine]-6,6″-dicarboxylic acid ligands bearing a thiol-reactive phenylsulfonyl group were conjugated to a protein that produces sizable PCSs [86]. A comprehensive survey of paramagnetic tags was provided by Miao and coworkers in 2022 [87].

5. Incorporation of Spin Labels and Paramagnetic Tags

5.1. AAC Reactions

5.1.1. Nitroxide Spin Labels

To realize in-cell DEER distance estimation, SDSL at two sites of green fluorescent protein (eGFP) was performed by the CuAAC reaction on double ncAA para-ethynylphenylalanine (pENF) mutants of eGFP with an azide derivative of a nitroxide spin label (3-(azidomethyl)-2,2,5,5-tetramethyl-1-pyrrolidinyloxyl, az-proxyl) (Figure 1) [88].

2′-N_3-G-modified guanosine-5′-triphosphate (GTP) was reacted with 4-(Prop-2-yn-1-ylamino)-2,2,6,6-tetramethylpiperidin-1-oxyl, a propargylated derivative of TEMPO, in the presence of tris-[(1 benzyl-1H-1,2,3-triazol-4-yl)methyl] amine (TBTA) complexed with Cu(I) to avoid in situ generation of Cu(I) [89]. Later, spin-labeled guanosine was attached to the 2′-OH group of internal adenosines in RNA through a DNA-catalyzed formation of a 2′,5′-phosphodiester bond. As displayed in Figure 2, 2′-triazolyl nitroxide spin labeling of DNA was performed for structural analysis by employing DEER experiments [90]. In this method, a 2′-alkynyl modification was introduced to the uridine units of Dickerson–Drew dodecamer variants, followed by reaction with an azide derivative of either TEMPO (5-Me) or (6-Me) to furnish spin-labeled duplexes 5 or 6. DEER-derived interspin distances are shown in panel B of Figure 2.

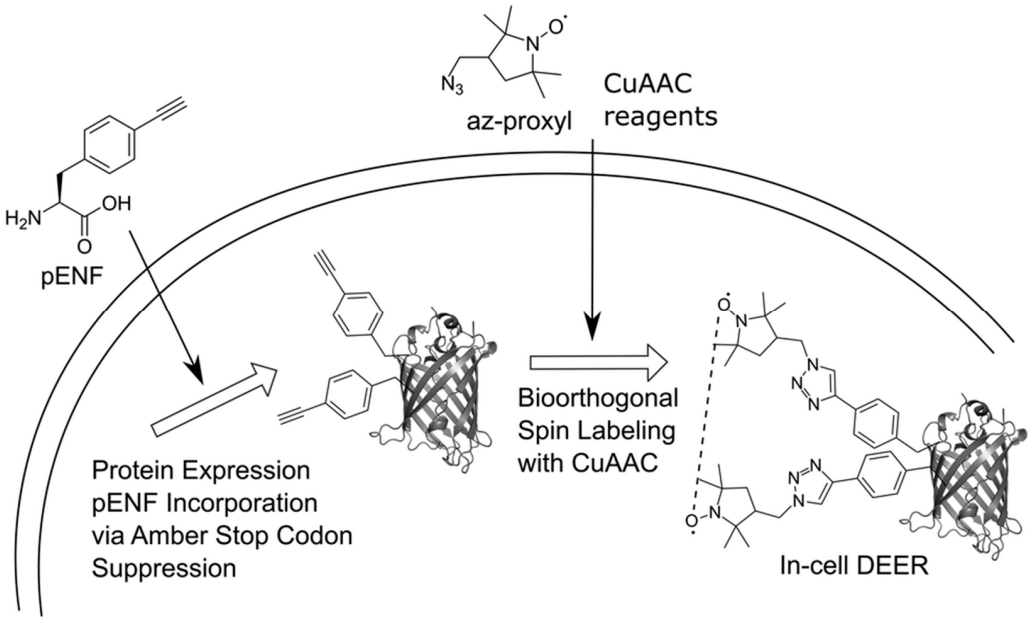


Figure 1. Schematic overview of the in vivo spin labeling approach via CuAAC followed by in-cell DEER distance determination. Reproduced from reference [88] under Creative Commons Attribution 3.0 Unported License.

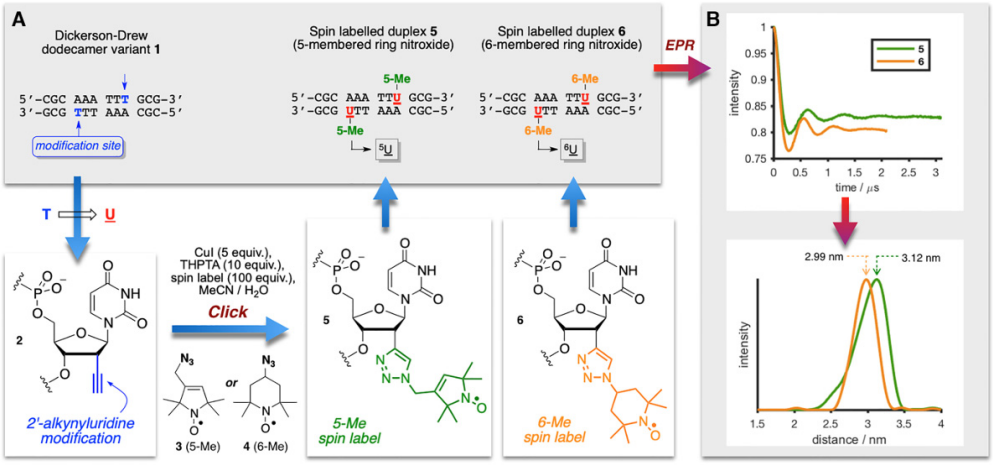
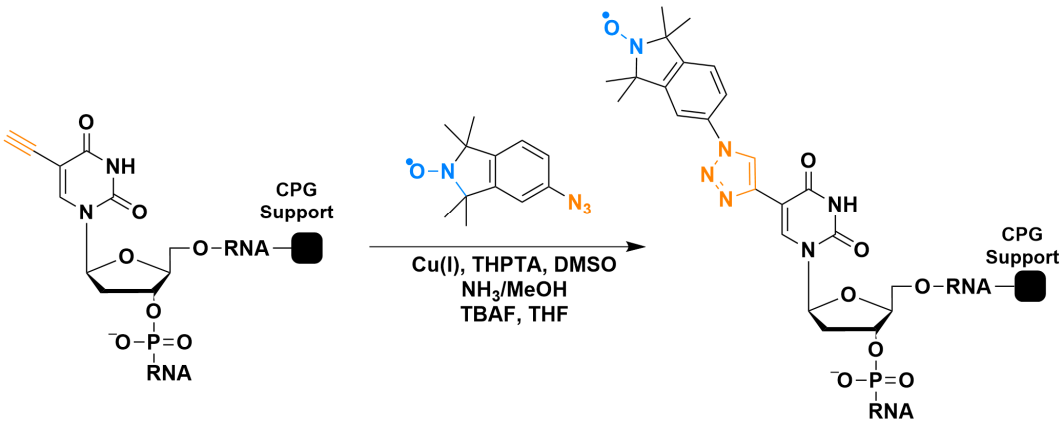


Figure 2. Synthesis of spin–labeled Dickerson–Drew dodecamer variants and DEER experiments. (**A**) Synthesis of spin-labeled DNA duplexes by modification of the 9-position in duplex **1** as a 2′-alkynyluridine (**2**), and incorporation of nitroxide radicals **3** (5-Me) and **4** (6-Me) into the spin–labeled duplexes **5** and **6**. (**B**) DEER-derived interspin distance distributions for duplexes **5** and **6** (200 µM ssDNA); the most probable interspin distances are 3.12 nm (**5**) and 2.99 nm (**6**). Data were analyzed using DeerAnalysis2016. Reproduced from reference [90] under Creative Commons CC BY license.

Similarly, five different nitroxide spin labels were site-specifically incorporated to DNA duplexes by means of CuAAC [91]. Interspin distances obtained from DEER experiments shed light on the structure and dynamics of the labeled DNA duplexes. Then, 25-mer parallel-stranded (ps) and antiparallel-stranded (aps) DNA conjugated with two spin labels were synthesized through the CuAAC reaction of 4-azido-2,2,6,6-tetramethylpiperidine-1-oxyl with 7-ethynyl-7-deaza-2′-deoxyadenosine or 5-ethynyl-2′-deoxyuridine. Interspin separations of spin-labeled residues obtained from PELDOR spectroscopy reveal differential positioning of spin labels in ps DNA with respect to aps DNA [92,93]. In another instance, the SDSL of DNA was accomplished by a CuAAC reaction of 5-ethynyl-2′-dU with an azide derivative of an isoindoline nitroxide radical. This SDSL DNA was subjected to EPR spectroscopy to elucidate local conformational changes in DNA [94]. The azide derivative

of the isoindoline nitroxide radical was clicked with ethynyl-bearing uracil and cytosine to furnish triazole-linked spin labels of the respective pyrimidines [95]. 5-Ethynyl-2′-dU-modified RNA was reacted with an azide-functionalized nitroxide radical solution in DMSO containing Cu(I) and tris(3-hydroxypropyltriazolylmethyl)-amine (THPTA) to furnish dU-spin-labeled RNA (Scheme 5) [96]. PELDOR measurements provided information on the distances between spin labels and the relative orientations of the spin labels.



Scheme 5. Spin labeling of RNA on CPG support with azide-functionalized nitroxide using CuAAC reaction.

Site-directed spin labeling of RNA was accomplished through the CuAAC reaction to enable the study of the conformations adopted by gem-diethyl and gem-dimethyl isoindoline nitroxide spin labels using PELDOR spectroscopy [97]. A nitroxide spin label, DBCO-SL, bearing a strained cyclic alkyne was synthesized for the SPAAC reaction with metabolically engineered glycans on the cell surface (Figure 3). EPR investigation on these spin-labeled glycans demonstrated distinct mobility of glycans in different cells [98]. Using a similar strategy, sialoglycans modified with C9-azido sialic acid were reacted with DBCO-SL via the SPAAC reaction to produce a spin-labeled cell surface that is ready for EPR spectroscopic investigations [99]. Subsequently, the same approach was extended to study the spin-labeled HeLa cells using EPR spectroscopy [100,101].

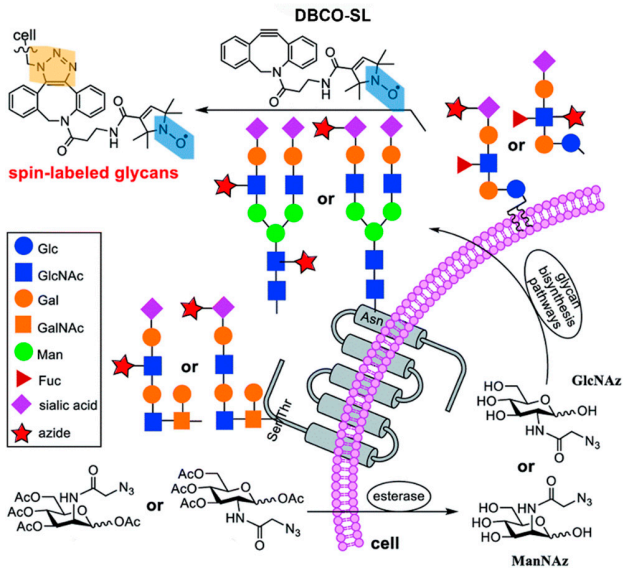


Figure 3. SPAAC reaction of DBCO-SL with metabolically engineered azido-glycans. Adapted with permission from reference [98] under Creative Commons Attribution 3.0 Unported License.

An alkyne-derivatized 1-oxyl 2,2,6,6-tetramethylpiperidine (TEMPO) spin label was tethered, via the CuAAC reaction, to the nanodiamond surface functionalized with silyl azides (ND-O-SiN_3) to study the dynamics of TEMPO radicals by X-band and 230 GHz EPR spectroscopy [102]. As depicted in Figure 4, silyl azide modification of hydroxylated nanodiamond was carried out in two steps, while an alkyne-derivatized TEMPO was obtained in a single step from 4-hydroxy-TEMPO. A dibenzocyclooctyne (DBCO) moiety bearing a TEMPO derivative was tethered to ND-O-SiN_3 employing SPAAC to facilitate high-frequency EPR for investigating the dynamics of TEMPO radicals in aqueous solution [103].

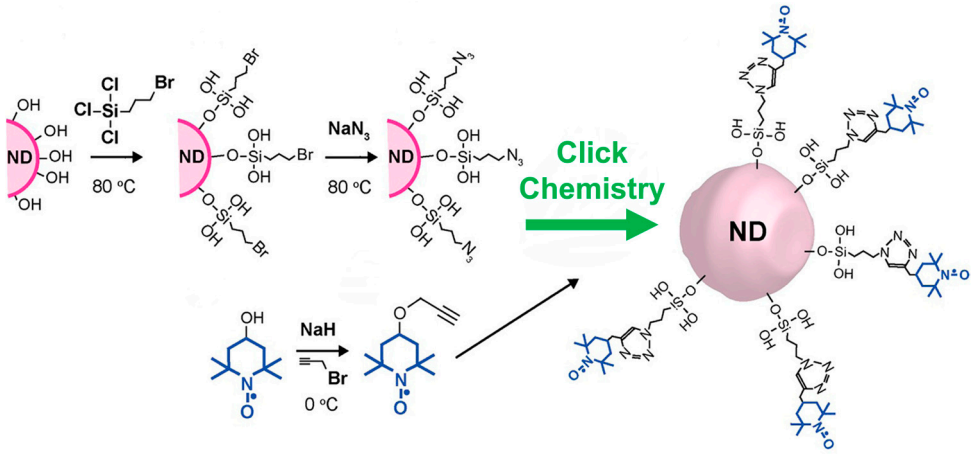
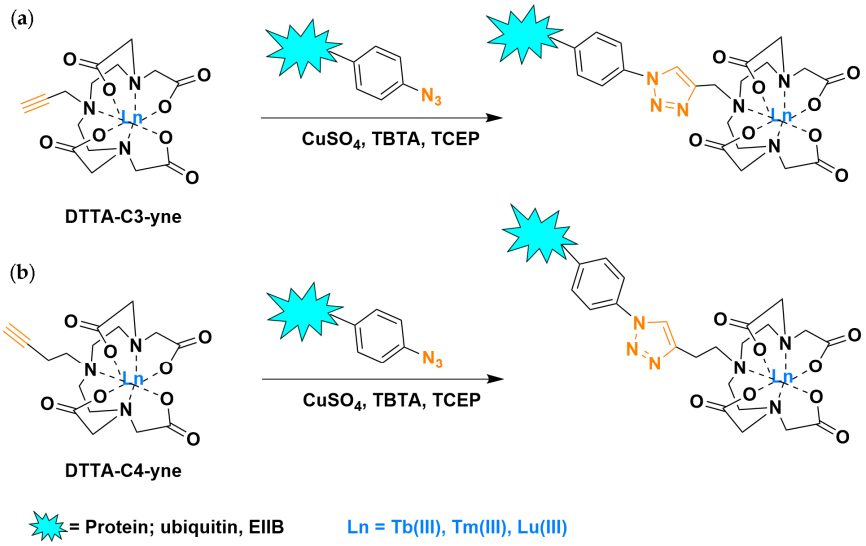


Figure 4. CuAAC approach for grafting TEMPO radicals on the ND surface. Reproduced with permission from reference [102].

5.1.2. Paramagnetic Metal Tags

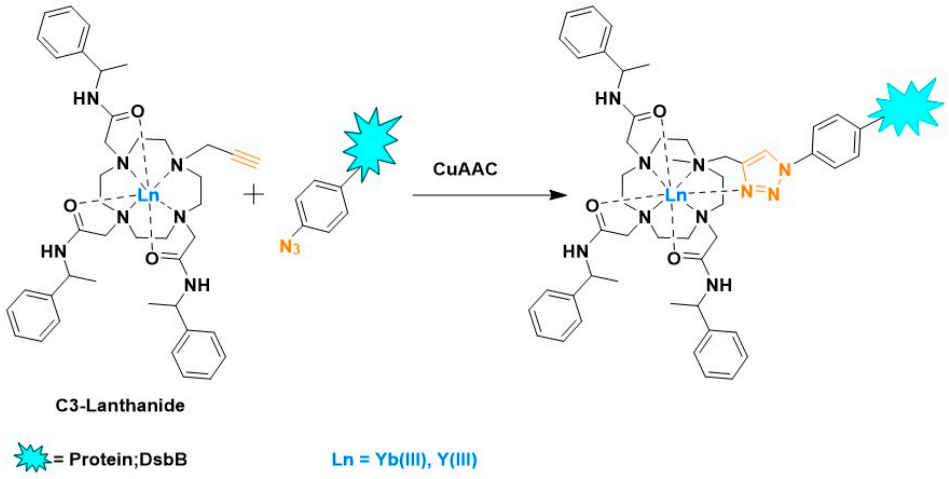
Iminodiacetic acid- and nitrilotriacetic acid-based lanthanide binding tags having alkyne functionalization were designed to conjugate through the CuAAC reactions with proteins—ubiquitin and GB1—comprising p-azido-l-phenylalanine mutations obtained by introducing an amber stop codon site-specifically in the gene of the target protein [104]. These click-modified mutants form complexes efficiently with lanthanide ions such as Tb(III), Tm(III), and Y(III), of which the first two afford the paramagnetic tags while the third delivers a diamagnetic tag. The Tb(III) and Tm(III) paramagnetic tags generated substantial PCSs.

As displayed in Scheme 6, lanthanide ion chelating moieties diethylene-triamine-tetraacetate propyl-1-yne (DTTA-C3-yne) and diethylene-triamine-tetraacetate butyl-1-yne (DTTA-C4-yne) were synthesized and clicked with p-azido-l-phenylalanine (*p*AzF) mutants of proteins ubiquitin and EIIB. $^{1}H–^{15}N$ hyperfine single quantum coherence (HSQC) NMR experiments with these conjugated mutants coordinated with paramagnetic Tb(III) and Tm(III), as well as diamagnetic Lu(III), allowed the extraction of PCS values [105]. Double-*p*AzF mutants of *E. coli* aspartate/glutamate binding protein (DEBP) were reacted with a C3–Gd(III) tag bearing an azide moiety via the CuAAC reaction to site-specifically position the Gd(III) spin label, thereby enabling distance measurements using W-band DEER spectroscopy [106].



Scheme 6. Schematic for attaching lanthanoid tags through unnatural amino acid pAzF. (**a**) DTTA-C3-yne or (**b**) DTTA-C4-yne reacts with the azide group of pAzF via CuAAC reaction.

1,4,7,10-tetraazacyclododecane (cyclen)-based C3-lanthanide tags comprising Yb(III) and Y(III) were attached to pAzF mutants of the disulfide bond formation protein B (DsbB), an α-helical integral membrane protein (IMP), via CuAAC (Scheme 7). These were subjected to ^{1}H-^{15}N TROSY-HSQC NMR spectroscopy to record pronounced PCSs [107].



Scheme 7. CuAAC reaction with pAzF DsbB mutant for attaching a paramagnetic cyclen-based C3-lanthanide tag.

Metal-based paramagnetic tags were introduced to RNA using a click chemistry protocol [82] to study RNA–protein interactions by paramagnetic NMR [108,109]. A macrocyclic cyclen ligand equipped with a terminal alkyne group was employed to coordinate metals such as Cu(II) and Co(II). The ^{15}N HSQC NMR spectra of NCp-RNA1 bearing a Cu(II)-cyclen paramagnetic tag and of NCp7-RNA2, which is unlabeled, the extent of attenuation of cross-peak intensities, and the protein backbone map are displayed in Figure 5. A metal ion chelator, ethylenediaminetetraacetic acid (EDTA), was tagged with tetrahyaluronans by employing click chemistry [110]. Paramagnetic tags were constructed by loading Mn(II) and Cu(II) ions onto this tag. These spin labels were employed to study the glycosaminoglycans (GAG) binding site of a signaling protein cytokine named interleukin-10 using PRE NMR. In this protocol, as shown in Scheme 8, tetrahyaluronan azide was reacted with N-propargyl-propaneamide in the presence of copper(II) sulfate, sodium ascorbate, and TBTA.

Next, nonasulfated tetrahyaluronanyl triazole was obtained by hydrolyzing the tetramethyl ester with 1N NaOH, followed by sulfation with the sulfur trioxide pyridine complex.

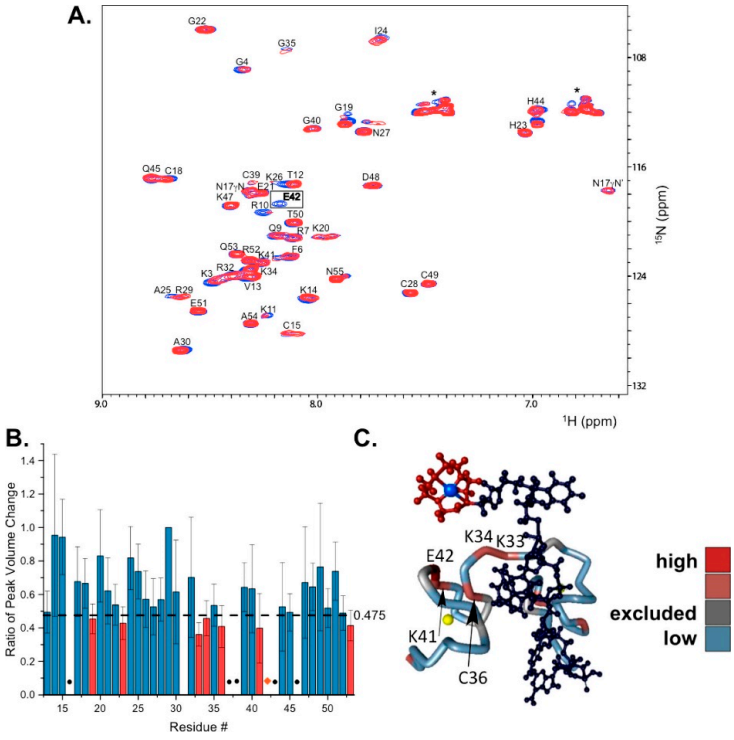
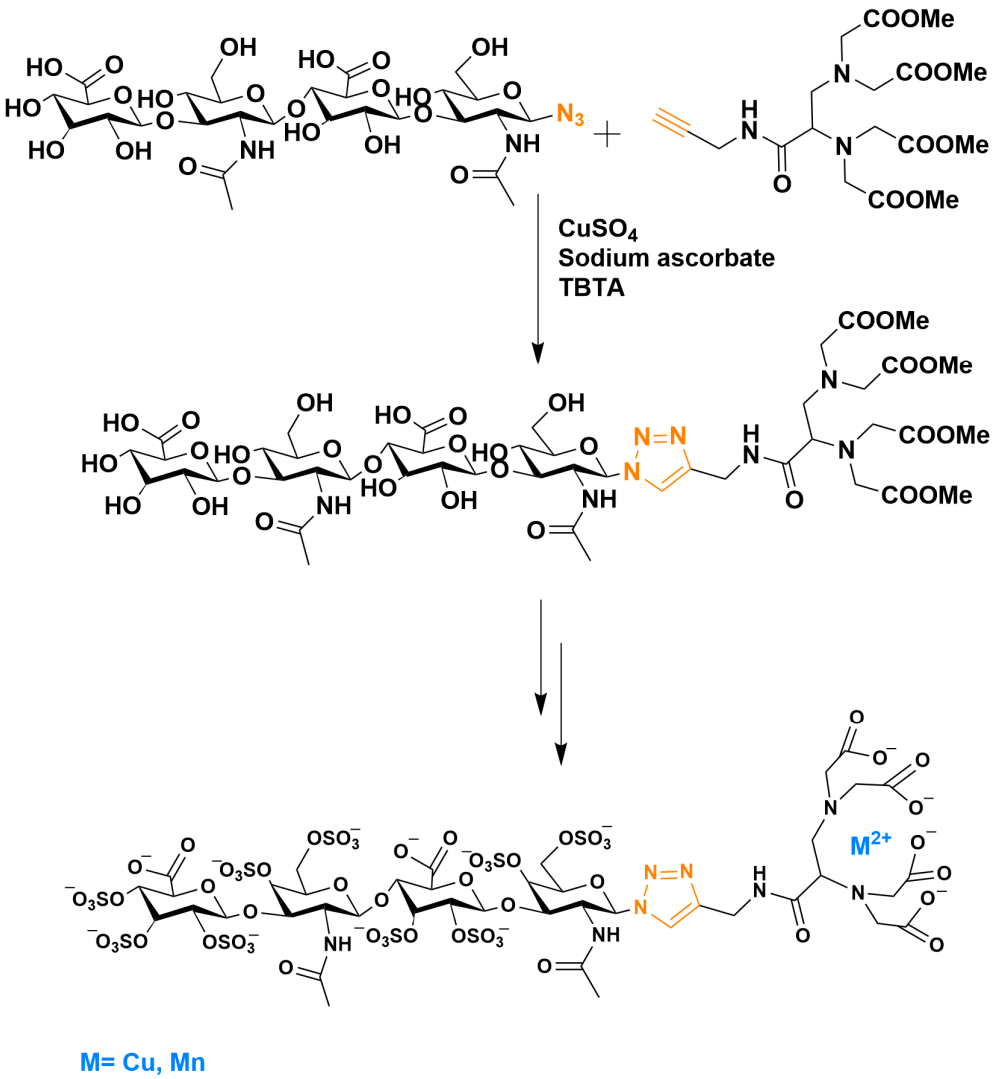
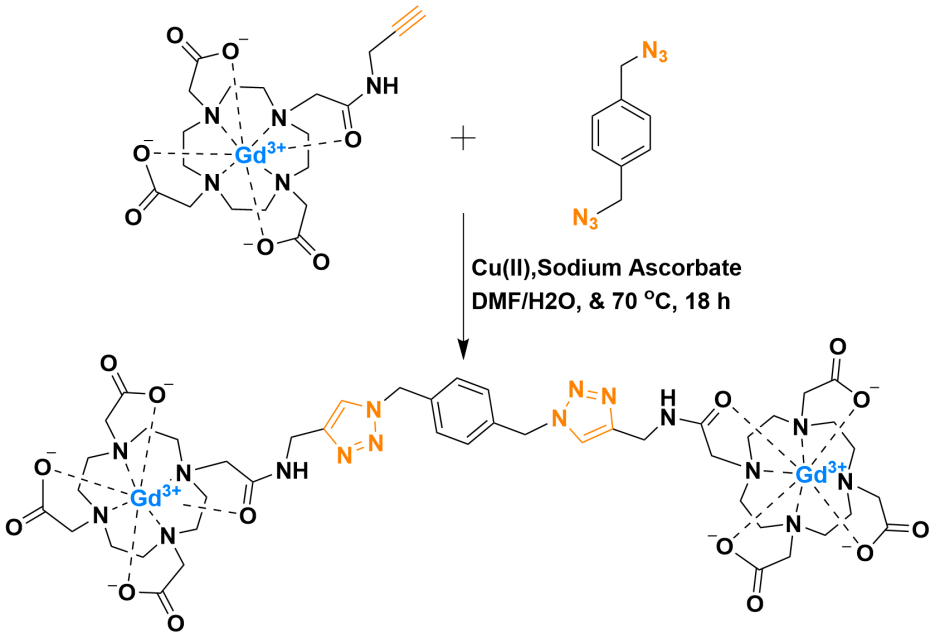


Figure 5. (**A**) The overlay of ^{1}H-^{15}N HSQC spectrum for NCp7-RNA 1 containing Cu(II)-cyclen paramagnetic tag (red) and NCp7-RNA 2, which is unlabeled (blue). The residue experiencing the strongest attenuation is shown in a box. Asterisks correspond to side chain amides. (**B**) Ratio of peak volume change in the cross-peak intensities. (•) Residues that are lowered in intensity upon binding the unlabeled **RNA 2** (F16, W37, K38, M46). They were excluded from the analysis. (◆) Residue (E42) that was excessively broadened due to proximity to **RNA 1** and also removed from the analysis. The horizontal line differentiates the residues experiencing the strongest attenuation. (**C**) Protein backbone map based on the previously reported NMR structure. The amino acid residues are color-coded based on the extent of attenuation of the HSQC cross-peak intensities. The yellow circles represent the two zinc atoms bound to zinc finger domains of the protein. Reproduced with permission from reference [109].

1,4,7,10-tetraazacyclododecane-1,4,7,10-tetraacetic acid (DOTA) is often referred to as the "gold standard" ligand [111] for chelating the trivalent gadolinium ion because of its ability to achieve eightfold coordination, thereby providing inherent kinetic inertness and stability to the Gd(III)–DOTA complex it forms. Gd(III)–DOTA complexes bearing an alkyne group were reacted with azide substrates such as trismethylazido benzene, hexakis(azidomethyl) benzene, and heptakis-6-azido-6-deoxy -β-cyclodextrin to furnish multimeric magnetic resonance contrast agents [112]. As shown in Scheme 9, two Gd(III)–DOTA complexes were stitched together into a single molecule having a flexible bistriazolebenzyl bridge as a spin label to explore distance measurements using DEER [113].

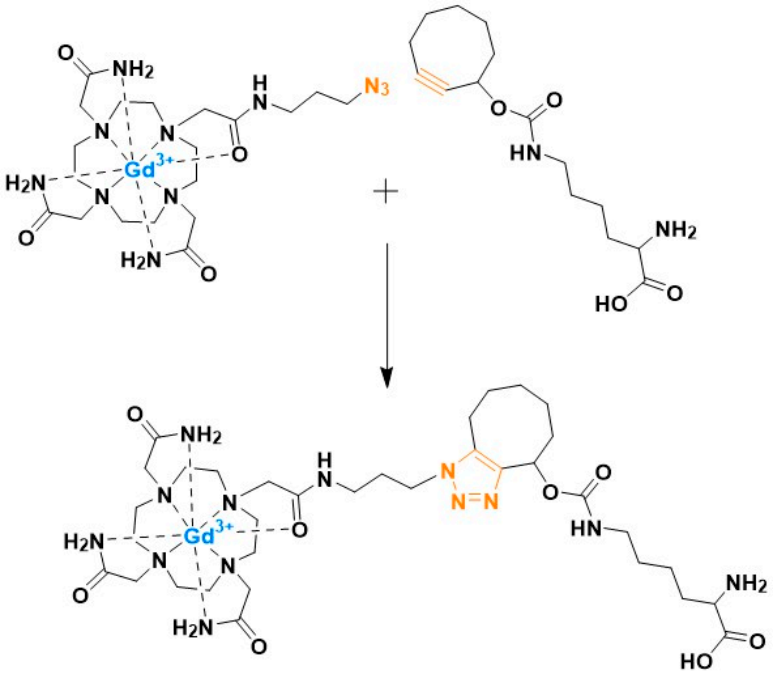


Scheme 8. Synthesis of nonasulfated tetrahyaluronanyl triazole paramagnetic tags.



Scheme 9. Bis-Gd(III)–DOTA with flexible bridge.

In another strategy illustrated in Scheme 10, an azide derivative of Gd-DOTAM (GDMA) was reacted with an ncAA, a strained-cyclooctyne (SCO)-derivatized L-lysine (ScoK), to obtain the SCO–Gd–DOTAM spin label [114]. This spin label was attached to the eGFP protein through a Y39ScoK mutation, followed by a SPAAC reaction with GDMA. The authors found that CuAAC of Y39PrK, in which Y39 is mutated to a propargyl-L-lysine, could not furnish sufficient labeling. Thus, SPAAC is the preferred strategy over CuAAC for labeling with a Gd spin label. The authors demonstrated that SPAAC could be performed in living E. coli cells, facilitating in-cell EPR detection and paving the way for protein dynamics studies in cells by employing DEER spectroscopy.



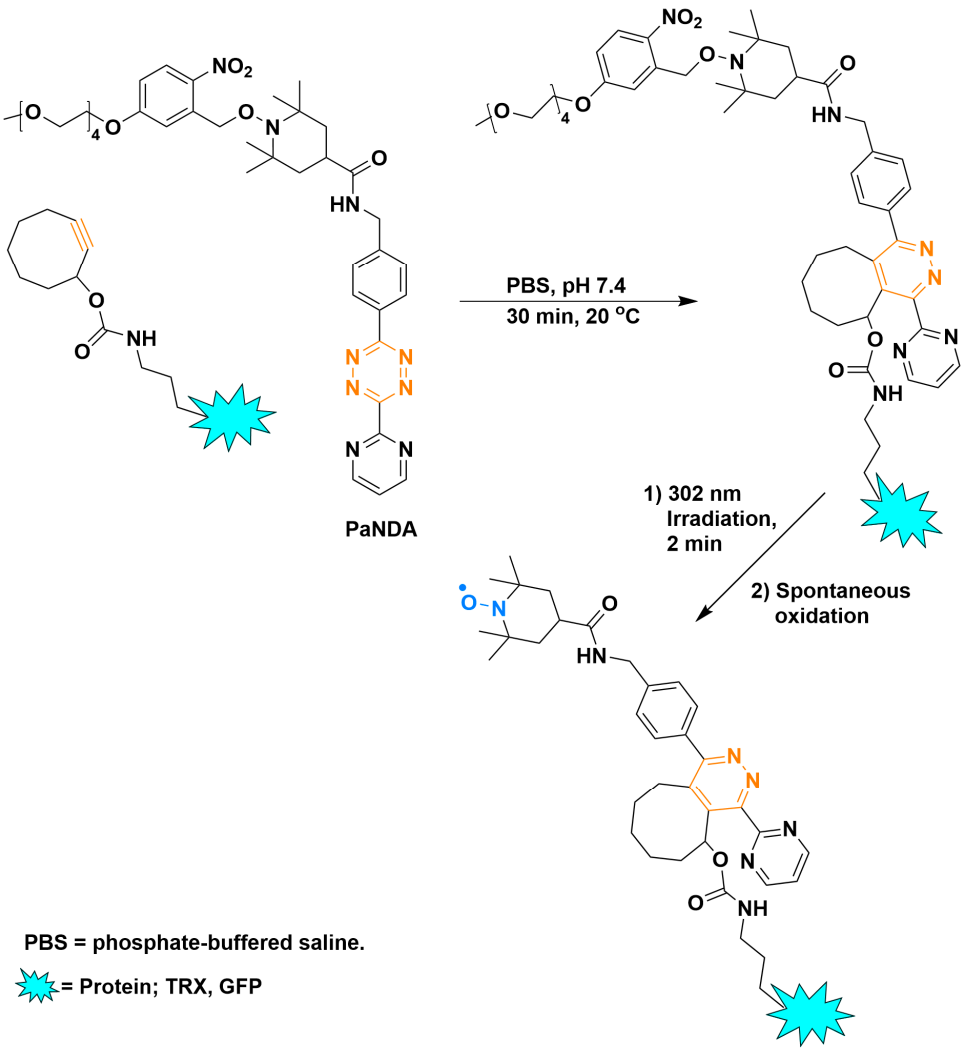
Scheme 10. Synthesis of SCO–Gd–DOTAM.

5.2. Diels–Alder Reaction

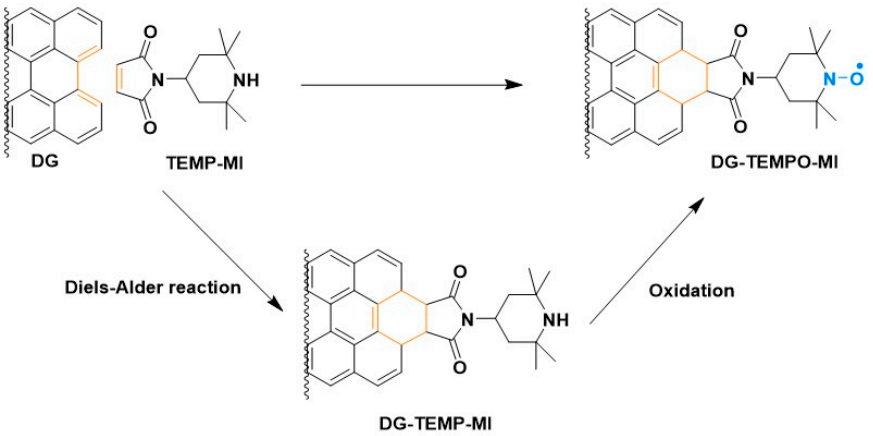
Nitroxide Spin Label

A tetraethyl-modified maleimido-PROXYL-based (PROXYL: 2,2,5,5-tetramethyl-1-pyrrolidinyloxy) spin label was introduced to proteins GFP and Escherichia coli oxidoreductase thioredoxin (TRX) via inverse-electron-demand Diels–Alder cycloaddition reaction (DAinv) [115]. In this protocol, a tetrazine moiety in the PaNDA spin label, containing an o-nitrobenzyl-protected TEMPO derivative, reacts with a cyclooctyne moiety incorporated into the protein to form pyridazine. Photodeprotection, followed by spontaneous oxidation, unmasks the TEMPO radical, as illustrated in Scheme 11.

The functionalization of graphene with the nitroxide radical was achieved via the Diels–Alder reaction [116]. As illustrated in Scheme 12, N-(2,2,6,6,-tetramethyl-4- piperidinyl) maleimide (TEMP-MI) was reacted with dispersed graphene (DG) to form the Diels–Alder adduct, which was then oxidized to DG-TEMPO-MI, a nitroxide radical. This redox-active material was analyzed by X-band EPR spectroscopy at different temperatures. Furthermore, W-band EPR spectroscopy was used to extract the individual hyperfine coupling constants of the nitrogen nucleus.



Scheme 11. Protein labeling with the photoactivatable nitroxide for DA_{inv} reaction.



Scheme 12. The Diels–Alder reaction of DG with TEMP-MI and the subsequent oxidation to DG-TEMPO-MI.

6. Summary and Outlook

In summary, this article presents a comprehensive portrait of the applications of cycloaddition reactions in tethering spin labels and paramagnetic tags. We have sought to capture the essence of the individual disciplines within this evolving interdisciplinary field under a single umbrella. As elaborated above, the CuAAC and SPAAC reactions have

been leveraged most for this purpose in biomolecular applications, while the Diels–Alder reaction has also been used sporadically in materials engineering. The integration of cycloaddition reactions with magnetic resonance has progressed considerably. However, a plethora of potent spin labels and paramagnetic tags remain untapped for bioconjugation through cycloaddition routes. Innovative designs of the azide and alkyne components of spin labels and paramagnetic tags would facilitate bioconjugation via the AAC reactions. Of particular interest are diethynyl-triazolyl-phosphine oxides (DTPOs) and ethynyl-ditriazolyl-phosphine oxides (EDPOs), recently obtained from triethynyl-phosphine oxide by employing the CuAAC reactions [117]. These reagents were used to afford a cyclic peptide–protein conjugate. DTPOs and EDPOs are promising candidates as putative linkers between biomolecules and spin labels and paramagnetic tags. In materials, the applications of cycloaddition reactions for functionalizing with spin labels and paramagnetic tags are rather scarce. We anticipate substantial progress in the deployment of the cycloaddition reactions, particularly the AAC reactions, as tools for conjugating spin labels and paramagnetic tags to materials in the coming years.

Author Contributions: Funding acquisition, S.-C.K.; Supervision, A.N.M. and S.-C.K.; Writing—original draft, A.N.M.; Writing—review and editing, A.N.M., A.K.M. and S.-C.K. All authors have read and agreed to the published version of the manuscript.

Funding: This work was financially supported by National Science and Technology Council, Taiwan (NSTC 112-2811-M-259-011-MY3).

Institutional Review Board Statement: Not applicable.

Informed Consent Statement: Not applicable.

Data Availability Statement: Not applicable.

Conflicts of Interest: The authors declare no conflicts of interest.

References

1. Nishiwaki, N. (Ed.) *Methods and Applications of Cycloaddition Reactions in Organic Syntheses*; John Wiley & Sons, Inc.: Hoboken, NJ, USA, 2014; pp. I–XII.
2. Porte, K.; Riomet, M.; Figliola, C.; Audisio, D.; Taran, F. Click and Bio-Orthogonal Reactions with Mesoionic Compounds. *Chem. Rev.* **2021**, *121*, 6718–6743. [CrossRef]
3. Yang, E.S.; Mapp, A.; Taylor, A.; Beer, P.D.; Goicoechea, J.M. Cyaphide-Azide 1,3-Dipolar Cycloaddition Reactions: Scope and Applicability. *Chem. Eur. J.* **2023**, *29*, e202301648. [CrossRef]
4. Moyano, A.; Rios, R. Asymmetric Organocatalytic Cyclization and Cycloaddition Reactions. *Chem. Rev.* **2011**, *111*, 4703–4832. [CrossRef]
5. Min, L.; Hu, Y.J.; Fan, J.H.; Zhang, W.; Li, C.C. Synthetic applications of type II intramolecular cycloadditions. *Chem. Soc. Rev.* **2020**, *49*, 7015–7043. [CrossRef] [PubMed]
6. Cai, W.Y.; Ding, Q.N.; Zhou, L.; Chen, J. Asymmetric Synthesis of Axially Chiral Molecules via Organocatalytic Cycloaddition and Cyclization Reactions. *Molecules* **2023**, *28*, 4306. [CrossRef] [PubMed]
7. Chiacchio, M.A.; Legnani, L. Density Functional Theory Calculations: A Useful Tool to Investigate Mechanisms of 1,3-Dipolar Cycloaddition Reactions. *Int. J. Mol. Sci.* **2024**, *25*, 1298. [CrossRef] [PubMed]
8. Shi, M.; Wei, Y.; Zhao, M.-X.; Zhang, J. *Organocatalytic Cycloadditions for Synthesis of Carbo- and Heterocycles*; Wiley-VCH Verlag GmbH & Co. KGaA: Weinheim, Germany, 2018.
9. Zhang, B.; Ge, H.M. Pericyclases for cycloaddition. *Natl. Sci. Rev.* **2022**, *9*, nwac229. [CrossRef]
10. Sankararaman, S. *Pericyclic Reactions—A Textbook: Reactions, Applications and Theory*; Wiley-VCH Verlag GmbH & Co. KGaA: Weinheim, Germany, 2005.
11. Kobayashi, S.; Jørgensen, K.A. *Cycloaddition Reactions in Organic Synthesis*; Wiley-VCH Verlag GmbH: Weinheim, Germany, 2002.
12. Breugst, M.; Reissig, H.U. The Huisgen Reaction: Milestones of the 1,3-Dipolar Cycloaddition. *Angew. Chem. Int. Ed.* **2020**, *59*, 12293–12307. [CrossRef]
13. Huisgen, R. 1,3-Dipolar Cycloadditions. Past and Future. *Angew. Chem. Int. Ed. Engl.* **1963**, *2*, 565–598. [CrossRef]
14. Pellissier, H. Asymmetric 1,3-dipolar cycloadditions. *Tetrahedron* **2007**, *63*, 3235–3285. [CrossRef]

15. Gothelf, K.V.; Jorgensen, K.A. Asymmetric 1,3-dipolar cycloaddition reactions. *Chem. Rev.* **1998**, *98*, 863–909. [CrossRef]
16. Rostovtsev, V.V.; Green, L.G.; Fokin, V.V.; Sharpless, K.B. A stepwise Huisgen cycloaddition process: Copper(I)-catalyzed regioselective "ligation" of azides and terminal alkynes. *Angew. Chem. Int. Ed.* **2002**, *41*, 2596–2599. [CrossRef]
17. Tornoe, C.W.; Christensen, C.; Meldal, M. Peptidotriazoles on solid phase: [1,2,3]-triazoles by regiospecific copper(I)-catalyzed 1,3-dipolar cycloadditions of terminal alkynes to azides. *J. Org. Chem.* **2002**, *67*, 3057–3064. [CrossRef]
18. Kolb, H.C.; Finn, M.G.; Sharpless, K.B. Click chemistry: Diverse chemical function from a few good reactions. *Angew. Chem. Int. Ed.* **2001**, *40*, 2004–2021. [CrossRef]
19. Hein, J.E.; Fokin, V.V. Copper-catalyzed azide-alkyne cycloaddition (CuAAC) and beyond: New reactivity of copper(I) acetylides. *Chem. Soc. Rev.* **2010**, *39*, 1302–1315. [CrossRef]
20. Abu-Orabi, S.T.; Atfah, M.A.; Jibril, I.; Mari'i, F.M.; Ali, A.A.-S. Dipolar cycloaddition reactions of organic azides with some acetylenic compounds. *J. Heterocycl. Chem.* **1989**, *26*, 1461–1468. [CrossRef]
21. Sletten, E.M.; Bertozzi, C.R. From Mechanism to Mouse: A Tale of Two Bioorthogonal Reactions. *Accounts Chem. Res.* **2011**, *44*, 666–676. [CrossRef] [PubMed]
22. Dresler, E.; Wolinski, P.; Wroblewska, A.; Jasinski, R. On the Question of Zwitterionic Intermediates in the [3+2] Cycloaddition Reactions between Aryl Azides and Ethyl Propiolate. *Molecules* **2023**, *28*, 8152. [CrossRef]
23. Agard, N.J.; Prescher, J.A.; Bertozzi, C.R. A strain-promoted [3+2] azide-alkyne cycloaddition for covalent modification of blomolecules in living systems. *J. Am. Chem. Soc.* **2004**, *126*, 15046–15047. [CrossRef] [PubMed]
24. Plass, T.; Milles, S.; Koehler, C.; Schultz, C.; Lemke, E.A. Genetically Encoded Copper-Free Click Chemistry. *Angew. Chem. Int. Ed.* **2011**, *50*, 3878–3881. [CrossRef]
25. Singh, I.; Heaney, F. Solid phase strain promoted "click" modification of DNA via [3+2]-nitrile oxide-cyclooctyne cycloadditions. *Chem. Commun.* **2011**, *47*, 2706–2708. [CrossRef]
26. Chang, P.V.; Prescher, J.A.; Sletten, E.M.; Baskin, J.M.; Miller, I.A.; Agard, N.J.; Lo, A.; Bertozzi, C.R. Copper-free click chemistry in living animals. *Proc. Natl. Acad. Sci. USA* **2010**, *107*, 1821–1826. [CrossRef]
27. Neef, A.B.; Schultz, C. Selective Fluorescence Labeling of Lipids in Living Cells. *Angew. Chem. Int. Ed.* **2009**, *48*, 1498–1500. [CrossRef]
28. The Nobel Prize in Chemistry. 2022. Available online: https://www.nobelprize.org/uploads/2022/10/press-chemistryprize2022-2.pdf (accessed on 13 October 2025).
29. Bauer, D.; Cornejo, M.A.; Hoang, T.T.; Lewis, J.S.; Zeglis, B.M. Click Chemistry and Radiochemistry: An Update. *Bioconjug. Chem.* **2023**, *34*, 1925–1950. [CrossRef]
30. Diels, O.; Alder, K. Synthesen in der hydroaromatischen Reihe. *Justus Liebigs Ann. Chem.* **1928**, *460*, 98–122. [CrossRef]
31. Houk, K.N.; Lin, Y.T.; Brown, F.K. Evidence for the concerted mechanism of the Diels-Alder reaction of butadiene with ethylene. *J. Am. Chem. Soc.* **1986**, *108*, 554–556. [CrossRef] [PubMed]
32. Linder, M.; Johansson, A.J.; Brinck, T. Mechanistic Insights into the Stepwise Diels-Alder Reaction of 4,6-Dinitrobenzofuroxan. *Org. Lett.* **2012**, *14*, 118–121. [CrossRef] [PubMed]
33. Jasinski, R. On the Question of Stepwise [4+2] Cycloaddition Reactions and Their Stereochemical Aspects. *Symmetry* **2021**, *13*, 1911. [CrossRef]
34. Domingo, L.R. Molecular Electron Density Theory: A Modern View of Reactivity in Organic Chemistry. *Molecules* **2016**, *21*, 1319. [CrossRef]
35. Domingo, L.R.; Pérez, P.; Sáez, J.A. Understanding the local reactivity in polar organic reactions through electrophilic and nucleophilic Parr functions. *RSC Adv.* **2013**, *3*, 1486–1494. [CrossRef]
36. Denis, P.A. Organic Chemistry of Graphene: The Diels-Alder Reaction. *Chem. Eur. J.* **2013**, *19*, 15719–15725. [CrossRef]
37. Sarkar, S.; Bekyarova, E.; Niyogi, S.; Haddon, R.C. Diels-Alder Chemistry of Graphite and Graphene: Graphene as Diene and Dienophile. *J. Am. Chem. Soc.* **2011**, *133*, 3324–3327. [CrossRef]
38. Cao, Y.; Osuna, S.; Liang, Y.; Haddon, R.C.; Houk, K.N. Diels-Alder Reactions of Graphene: Computational Predictions of Products and Sites of Reaction. *J. Am. Chem. Soc.* **2013**, *135*, 17643–17649. [CrossRef]
39. Ji, Z.; Chen, J.; Huang, L.; Shi, G.Q. High-yield production of highly conductive graphene via reversible covalent chemistry. *Chem. Commun.* **2015**, *51*, 2806–2809. [CrossRef] [PubMed]
40. Seo, J.M.; Jeon, I.Y.; Baek, J.B. Mechanochemically driven solid-state Diels-Alder reaction of graphite into graphene nanoplatelets. *Chem. Sci.* **2013**, *4*, 4273–4277. [CrossRef]
41. Weil, J.A.; Bolton, J.R. *Electron Pramagnetic Resonance: Elementary Theory and Practical Applications*, 2nd ed.; John Wiley & Sons, Inc.: New York, NY, USA, 2007.
42. Eaton, G.R.; Eaton, S.S.E.; Salikhov, K.M. *Foundations of Modern EPR*; World Scientific Publishing Company: Hackensack, NJ, USA, 1998.
43. Harriman, J.E. *Theoretical Foundations of Electron Spin Resonance*; Academic Press, Inc.: New York, NY, USA, 1978.
44. Abragam, A.; Bleaney, B. *Electron Paramagnetic Resonance of Transition Ions*; Oxford University Press: Oxford, UK, 2012.

45. Poole, C.P. *Electron Spin Resonance: A Comprehensive Treatise on Experimental Techniques*; Dover Publications, Inc.: New York, NY, USA, 1996.
46. Palmer, G. Electron Paramagnetic Resonance of Metalloproteins. In *Physical Methods in Bioorganic Chemistry: Spectroscopy and Magnetism*; Que, L., Ed.; University Science Books: Sausalito, CA, USA, 2000; pp. 121–185.
47. Banerjee, R. Radical Enzymology. *Chem. Rev.* **2003**, *103*, 2081–2456. [CrossRef]
48. Pilbrow, J.R. EPR of B_{12}-Dependent Enzyme Reactions and Related Systems. In *B_{12}*; Dolphin, D., Ed.; John Wiley & Sons: New York, NY, USA, 1982; Volume 1, pp. 431–462.
49. Gerfen, G.J. EPR Spectroscopy of B_{12}-Dependent Enzymes. In *Chemistry and Biochemistry of B_{12}*; Banerjee, R., Ed.; John Wiley & Sons, Inc.: New York, NY, USA, 1999; pp. 165–195.
50. Schweiger, A.; Jeschke, G. *Principles of Pulse Electron Paramagnetic Resonance*; Oxford University Press: Oxford, UK, 2001.
51. Fanucci, G.E.; Cafiso, D.S. Recent advances and applications of site-directed spin labeling. *Curr. Opin. Struc. Biol.* **2006**, *16*, 644–653. [CrossRef]
52. Jeschke, G. Distance measurements in the nanometer range by pulse EPR. *ChemPhysChem* **2002**, *3*, 927–932. [CrossRef]
53. Jeschke, G.; Polyhach, Y. Distance measurements on spin-labelled biomacromolecules by pulsed electron paramagnetic resonance. *Phys. Chem. Chem. Phys.* **2007**, *9*, 1895–1910. [CrossRef]
54. Eaton, S.S.; Eaton, G.R. Multifrequency Pulsed EPR and the Characterization of Molecular Dynamics. *Method. Enzymol.* **2015**, *563*, 37–58. [CrossRef]
55. Ledwitch, K.; Künze, G.; Okwei, E.; Sala, D.; Meiler, J. Non-canonical amino acids for site-directed spin labeling of membrane proteins. *Curr. Opin. Struc. Biol.* **2024**, *89*, 102936. [CrossRef]
56. Sahu, I.D.; Lorigan, G.A. Electron Paramagnetic Resonance as a Tool for Studying Membrane Proteins. *Biomolecules* **2020**, *10*, 763. [CrossRef] [PubMed]
57. Klare, J.P.; Steinhoff, H.J. Spin labeling EPR. *Photosynth. Res.* **2009**, *102*, 377–390. [CrossRef]
58. Jeschke, G.; Chechik, V.; Ionita, P.; Godt, A.; Zimmermann, H.; Banham, J.; Timmel, C.R.; Hilger, D.; Jung, H. DeerAnalysis2006—A comprehensive software package for analyzing pulsed ELDOR data. *Appl. Magn. Reson.* **2006**, *30*, 473–498. [CrossRef]
59. Thwaites, J.D.; Bertini, I.; Sacconi, L. Proton Resonance Studies of the Solution Equilibria of Nickel(II) Complexes with Schiff Bases Formed from Salicylaldehydes and N,N-Substituted Ethylenediamines. II. *Inorg. Chem.* **1966**, *5*, 1036–1041. [CrossRef]
60. Thwaites, J.D.; Sacconi, L. Proton Resonance Studies of the Solution Equilibria of Nickel(II)Complexes with Schiff Bases Formed from Salicylaldehydes and N,N-Substituted Ethylenediamines. *I. Inorg. Chem.* **1966**, *5*, 1029–1035. [CrossRef]
61. Banci, L.; Piccioli, M.; Scozzafava, A. Advances in the NMR investigation of paramagnetic molecules in solution. *Coord. Chem. Rev.* **1992**, *120*, 1–28. [CrossRef]
62. Lehr, M.; Paschelke, T.; Trumpf, E.; Vogt, A.M.; Näther, C.; Sönnichsen, F.D.; McConnell, A.J. A Paramagnetic NMR Spectroscopy Toolbox for the Characterisation of Paramagnetic/Spin-Crossover Coordination Complexes and Metal-Organic Cages. *Angew. Chem. Int. Ed.* **2020**, *59*, 19344–19351. [CrossRef]
63. Ravera, E.; Gigli, L.; Fiorucci, L.; Luchinat, C.; Parigi, G. The evolution of paramagnetic NMR as a tool in structural biology. *Phys. Chem. Chem. Phys.* **2022**, *24*, 17397–17416. [CrossRef]
64. Columbus, L.; Kroncke, B. Solution NMR Structure Determination of Polytopic α-Helical Membrane Proteins: A Guide to Spin Label Paramagnetic Relaxation Enhancement Restraints. *Membr. Proteins Eng. Purif. Cryst.* **2015**, *557*, 329–348. [CrossRef]
65. Gottstein, D.; Reckel, S.; Dötsch, V.; Güntert, P. Requirements on Paramagnetic Relaxation Enhancement Data for Membrane Protein Structure Determination by NMR. *Structure* **2012**, *20*, 1019–1027. [CrossRef]
66. Maity, A.N.; Chen, J.-R.; Ke, S.-C. Exploring the mechanism of action of lysine 5,6-aminomutase using EPR and ENDOR spectroscopies. *Methods Enzymol.* **2022**, *669*, 197–228. [CrossRef] [PubMed]
67. Maity, A.N.; Chen, J.-R.; Li, Q.-Y.; Ke, S.-C. The Nitrogen Atom of Vitamin B6 Is Essential for the Catalysis of Radical Aminomutases. *Int. J. Mol. Sci.* **2022**, *23*, 5210. [CrossRef] [PubMed]
68. Maity, A.N.; Chen, J.R.; Ke, T.X.; Ke, S.C. 5-Hydroxylysine Captures the Suicidally-Inactivated Conformational State of Lysine 5,6-Aminomutase. *Int. J. Mol. Sci.* **2025**, *26*, 8561. [CrossRef]
69. Maity, A.N.; Chen, Y.H.; Ke, S.C. Large-scale domain motions and pyridoxal-5′-phosphate assisted radical catalysis in coenzyme B_{12}-dependent aminomutases. *Int. J. Mol. Sci.* **2014**, *15*, 3064–3087. [CrossRef] [PubMed]
70. Maity, A.N.; Hsieh, C.P.; Huang, M.H.; Chen, Y.H.; Tang, K.H.; Behshad, E.; Frey, P.A.; Ke, S.C. Evidence for conformational movement and radical mechanism in the reaction of 4-thia-L-lysine with lysine 5,6-aminomutase. *J. Phys. Chem. B* **2009**, *113*, 12161–12163. [CrossRef]
71. Chen, J.-R.; Ke, T.-X.; Frey, P.A.; Ke, S.-C. Electron Spin Echo Envelope Modulation Spectroscopy Reveals How Adenosylcobalamin-Dependent Lysine 5,6-Aminomutase Positions the Radical Pair Intermediates and Modulates Their Stabilities for Efficient Catalysis. *ACS Catal.* **2021**, *11*, 14352–14368. [CrossRef]

72. Chen, Y.H.; Maity, A.N.; Frey, P.A.; Ke, S.C. Mechanism-based inhibition reveals transitions between two conformational states in the action of lysine 5,6-aminomutase: A combination of electron paramagnetic resonance spectroscopy, electron nuclear double resonance spectroscopy, and density functional theory study. *J. Am. Chem. Soc.* **2013**, *135*, 788–794. [CrossRef]
73. Chen, Y.H.; Maity, A.N.; Pan, Y.C.; Frey, P.A.; Ke, S.C. Radical stabilization is crucial in the mechanism of action of lysine 5,6-aminomutase: Role of tyrosine-263α as revealed by electron paramagnetic resonance spectroscopy. *J. Am. Chem. Soc.* **2011**, *133*, 17152–17155. [CrossRef]
74. Reed, G.H.; Mansoorabadi, S.O. The positions of radical intermediates in the active sites of adenosylcobalamin-dependent enzymes. *Curr. Opin. Struc. Biol.* **2003**, *13*, 716–721. [CrossRef]
75. Maity, A.N.; Lin, H.H.; Chiang, H.S.; Lo, H.H.; Ke, S.C. Reaction of pyridoxal-5′-phosphate-*N*-oxide with lysine 5,6-aminomutase: Enzyme flexibility toward cofactor analog. *ACS Catal.* **2015**, *5*, 3093–3099. [CrossRef]
76. Lo, H.H.; Lin, H.H.; Maity, A.N.; Ke, S.C. The molecular mechanism of the open-closed protein conformational cycle transitions and coupled substrate binding, activation and product release events in lysine 5,6-aminomutase. *Chem. Commun.* **2016**, *52*, 6399–6402. [CrossRef] [PubMed]
77. Piccioli, M. Paramagnetic NMR Spectroscopy Is a Tool to Address Reactivity, Structure, and Protein-Protein Interactions of Metalloproteins: The Case of Iron-Sulfur Proteins. *Magnetochemistry* **2020**, *6*, 46. [CrossRef]
78. Li, H.; Sun, H. NMR Studies of Metalloproteins. In *NMR of Proteins and Small Biomolecules*; Zhu, G., Ed.; Springer: Berlin/Heidelberg, Germany, 2012; pp. 69–98.
79. Ravera, E.; Gigli, L.; Suturina, E.A.; Calderone, V.; Fragai, M.; Parigi, G.; Luchinat, C. A High-Resolution View of the Coordination Environment in a Paramagnetic Metalloprotein from its Magnetic Properties. *Angew. Chem. Int. Ed.* **2021**, *60*, 14960–14966. [CrossRef]
80. Braun, T.; Drescher, M.; Summerer, D. Expanding the Genetic Code for Site-Directed Spin-Labeling. *Int. J. Mol. Sci.* **2019**, *20*, 373. [CrossRef]
81. Schmidt, M.J.; Borbas, J.; Drescher, M.; Summerer, D. A Genetically Encoded Spin Label for Electron Paramagnetic Resonance Distance Measurements. *J. Am. Chem. Soc.* **2014**, *136*, 1238–1241. [CrossRef] [PubMed]
82. Paredes, E.; Das, S.R. Click Chemistry for Rapid Labeling and Ligation of RNA. *ChemBioChem* **2011**, *12*, 125–131. [CrossRef]
83. Shelke, S.A.; Sigurdsson, S.T. Site-Directed Spin Labeling for EPR Studies of Nucleic Acids. In *Modified Nucleic Acids*; Nakatani, K., Tor, Y., Eds.; Springer International Publishing: Cham, Switzerland, 2016; pp. 159–187.
84. Columbus, L.; Hubbell, W.L. A new spin on protein dynamics. *Trends Biochem. Sci.* **2002**, *27*, 288–295. [CrossRef]
85. Roser, P.; Schmidt, M.J.; Drescher, M.; Summerer, D. Site-directed spin labeling of proteins for distance measurements in vitro and in cells. *Org. Biomol. Chem.* **2016**, *14*, 5468–5476. [CrossRef] [PubMed]
86. Li, M.H.; Zhang, X.; Pan, B.B.; Su, X.C. Excellent Fe(II) Binding Tag in Protein Paramagnetic NMR Spectroscopy. *Inorg. Chem.* **2025**, *64*, 7890–7901. [CrossRef]
87. Miao, Q.; Nitsche, C.; Orton, H.; Overhand, M.; Otting, G.; Ubbink, M. Paramagnetic Chemical Probes for Studying Biological Macromolecules. *Chem. Rev.* **2022**, *122*, 9571–9642. [CrossRef] [PubMed]
88. Widder, P.; Schuck, J.; Summerer, D.; Drescher, M. Combining site-directed spin labeling and in-cell EPR distance determination. *Phys. Chem. Chem. Phys.* **2020**, *22*, 4875–4879. [CrossRef] [PubMed]
89. Büttner, L.; Javadi-Zarnaghi, F.; Höbartner, C. Site-Specific Labeling of RNA at Internal Ribose Hydroxyl Groups: Terbium-Assisted Deoxyribozymes at Work. *J. Am. Chem. Soc.* **2014**, *136*, 8131–8137. [CrossRef]
90. Hardwick, J.S.; Haugland, M.M.; El-Sagheer, A.H.; Ptchelkine, D.; Beierlein, F.R.; Lane, A.N.; Brown, T.; Lovett, J.E.; Anderson, E.A. 2′-Alkynyl spin-labelling is a minimally perturbing tool for DNA structural analysis. *Nucleic Acids Res.* **2020**, *48*, 2830–2840. [CrossRef]
91. Haugland, M.M.; El-Sagheer, A.H.; Porter, R.J.; Peña, J.; Brown, T.; Anderson, E.A.; Lovett, J.E. 2′-Alkynylnucleotides: A Sequence- and Spin Label-Flexible Strategy for EPR Spectroscopy in DNA. *J. Am. Chem. Soc.* **2016**, *138*, 9069–9072. [CrossRef]
92. Wunnicke, D.; Ding, P.; Yang, H.Z.; Seela, F.; Steinhoff, H.J. DNA with Parallel Strand Orientation: A Nanometer Distance Study with Spin Labels in the Watson-Crick and the Reverse Watson-Crick Double Helix. *J. Phys. Chem. B* **2015**, *119*, 13593–13599. [CrossRef]
93. Ding, P.; Wunnicke, D.; Steinhoff, H.J.; Seela, F. Site-Directed Spin-Labeling of DNA by the Azide-Alkyne 'Click' Reaction: Nanometer Distance Measurements on 7-Deaza-2′-deoxyadenosine and 2′-Deoxyuridine Nitroxide Conjugates Spatially Separated or Linked to a 'dA-dT' Base Pair. *Chem. Eur. J.* **2010**, *16*, 14385–14396. [CrossRef] [PubMed]
94. Jakobsen, U.; Shelke, S.A.; Vogel, S.; Sigurdsson, S.T. Site-Directed Spin-Labeling of Nucleic Acids by Click Chemistry: Detection of Abasic Sites in Duplex DNA by EPR Spectroscopy. *J. Am. Chem. Soc.* **2010**, *132*, 10424–10428. [CrossRef]
95. Shelke, S.A.; Sandholt, G.B.; Sigurdsson, S.T. Nitroxide-labeled pyrimidines for non-covalent spin-labeling of abasic sites in DNA and RNA duplexes. *Org. Biomol. Chem.* **2014**, *12*, 7366–7374. [CrossRef]
96. Kerzhner, M.; Abdullin, D.; Wiecek, J.; Matsuoka, H.; Hagelueken, G.; Schiemann, O.; Famulok, M. Post-synthetic Spin-Labeling of RNA through Click Chemistry for PELDOR Measurements. *Chem. Eur. J.* **2016**, *22*, 12113–12121. [CrossRef]

97. Wuebben, C.; Blume, S.; Abdullin, D.; Brajtenbach, D.; Haege, F.; Kath-Schorr, S.; Schiemann, O. Site-Directed Spin Labeling of RNA with a *Gem*-Diethylisoindoline Spin Label: PELDOR, Relaxation, and Reduction Stability. *Molecules* **2019**, *24*, 4482. [CrossRef]
98. Jaiswal, M.; Tran, T.T.; Li, Q.J.; Yan, X.; Zhou, M.W.; Kundu, K.; Fanucci, G.E.; Guo, Z.W. A metabolically engineered spin-labeling approach for studying glycans on cells. *Chem. Sci.* **2020**, *11*, 12522–12532. [CrossRef]
99. Jaiswal, M.; Tran, T.T.; Guo, J.T.; Zhou, M.W.; Diaz, J.G.; Fanucci, G.E.; Guo, Z.W. Enzymatic glycoengineering-based spin labelling of cell surface sialoglycans to enable their analysis by electron paramagnetic resonance (EPR) spectroscopy. *Analyst* **2022**, *147*, 784–788. [CrossRef]
100. Jaiswal, M.; Tran, T.T.; Guo, J.T.; Zhou, M.W.; Kundu, S.; Guo, Z.W.; Fanucci, G.E. Spin-Labeling Insights into How Chemical Fixation Impacts Glycan Organization on Cells. *Appl. Magn. Reson.* **2024**, *55*, 317–333. [CrossRef] [PubMed]
101. Jaiswal, M.; Zhou, M.W.; Guo, J.T.; Tran, T.T.; Kundu, S.; Jaufer, A.M.; Fanucci, G.E.; Guo, Z.W. Different Biophysical Properties of Cell Surface α2,3-and α2,6-Sialoglycans Revealed by Electron Paramagnetic Resonance Spectroscopic Studies. *J. Phys. Chem. B* **2023**, *127*, 1749–1757. [CrossRef] [PubMed]
102. Romanova, E.E.; Akiel, R.; Cho, F.H.; Takahashi, S. Grafting Nitroxide Radicals on Nanodiamond Surface Using Click Chemistry. *J. Phys. Chem. A* **2013**, *117*, 11933–11939. [CrossRef]
103. Akiel, R.D.; Stepanov, V.; Takahashi, S. High-Frequency Electron Paramagnetic Resonance Spectroscopy of Nitroxide-Functionalized Nanodiamonds in Aqueous Solution. *Cell Biochem. Biophys.* **2017**, *75*, 151–157. [CrossRef]
104. Loh, C.T.; Graham, B.; Abdelkader, E.H.; Tuck, K.L.; Otting, G. Generation of Pseudocontact Shifts in Proteins with Lanthanides Using Small "Clickable" Nitrilotriacetic Acid and Iminodiacetic Acid Tags. *Chem. Eur. J.* **2015**, *21*, 5084–5092. [CrossRef] [PubMed]
105. Jiang, W.X.; Gu, X.H.; Dong, X.; Tang, C. Lanthanoid tagging via an unnatural amino acid for protein structure characterization. *J. Biomol. NMR* **2017**, *67*, 273–282. [CrossRef]
106. Abdelkader, E.H.; Feintuch, A.; Yao, X.; Adams, L.A.; Aurelio, L.; Graham, B.; Goldfarb, D.; Otting, G. Protein conformation by EPR spectroscopy using gadolinium tags clicked to genetically encoded *p*-azido-L-phenylalanine. *Chem. Commun.* **2015**, *51*, 15898–15901. [CrossRef]
107. Ledwitch, K.V.; Künze, G.; McKinney, J.R.; Okwei, E.; Larochelle, K.; Pankewitz, L.; Ganguly, S.; Darling, H.L.; Coin, I.; Meiler, J. Sparse pseudocontact shift NMR data obtained from a non-canonical amino acid-linked lanthanide tag improves integral membrane protein structure prediction. *J. Biomol. NMR* **2023**, *77*, 69–82. [CrossRef]
108. Seebald, L.M.; DeMott, C.M.; Ranganathan, S.; Asare-Okai, P.N.; Glazunova, A.; Chen, A.; Shekhtman, A.; Royzen, M. Cobalt-based paramagnetic probe to study RNA-protein interactions by NMR. *J. Inorg. Biochem.* **2017**, *170*, 202–208. [CrossRef] [PubMed]
109. Seebald, L.M.; DeMott, C.M.; Ranganathan, S.; Asare-Okai, P.N.; Glazunova, A.; Chen, A.; Shekhtman, A.; Royzen, M. Cu(II)-Based Paramagnetic Probe to Study RNA Protein Interactions by NMR. *Inorg. Chem.* **2017**, *56*, 3773–3780. [CrossRef]
110. Köhling, S.; Künze, G.; Lemmnitzer, K.; Bermudez, M.; Wolber, G.; Schiller, J.; Huster, D.; Rademann, J. Chemoenzymatic Synthesis of Nonasulfated Tetrahyaluronan with a Paramagnetic Tag for Studying Its Complex with Interleukin-10. *Chem. Eur. J.* **2016**, *22*, 5563–5574. [CrossRef] [PubMed]
111. Huynh, P.T.; Vu, H.D.; Ryu, J.; Kim, H.S.; Jung, H.S.; Youn, S.W. Gadolinium-Cyclic 1,4,7,10-Tetraazacyclododecane-1,4,7,10-Tetraacetic Acid-Click-Sulfonyl Fluoride for Probing Serine Protease Activity in Magnetic Resonance Imaging. *Molecules* **2023**, *28*, 3538. [CrossRef]
112. Song, Y.; Kohlmeir, E.K.; Meade, T.J. Synthesis of multimeric MR contrast agents for cellular imaging. *J. Am. Chem. Soc.* **2008**, *130*, 6662–6663. [CrossRef] [PubMed]
113. Potapov, A.; Song, Y.; Meade, T.J.; Goldfarb, D.; Astashkin, A.V.; Raitsimring, A. Distance measurements in model bis-Gd(III) complexes with flexible "bridge". Emulation of biological molecules having flexible structure with Gd(III) labels attached. *J. Magn. Reson.* **2010**, *205*, 38–49. [CrossRef]
114. Kucher, S.; Korneev, S.; Klare, J.P.; Klose, D.; Steinhoff, H.J. *In cell* Gd^{3+}-based site-directed spin labeling and EPR spectroscopy of eGFP. *Phys. Chem. Chem. Phys.* **2020**, *22*, 13358–13362. [CrossRef]
115. Kugele, A.; Silkenath, B.; Langer, J.; Wittmann, V.; Drescher, M. Protein Spin Labeling with a Photocaged Nitroxide Using Diels-Alder Chemistry. *ChemBioChem* **2019**, *20*, 2479–2484. [CrossRef]

116. Lazar, I.M.; Rostas, A.M.; Straub, P.S.; Schleicher, E.; Weber, S.; Mülhaupt, R. Simple Covalent Attachment of Redox-Active Nitroxyl Radicals to Graphene via Diels-Alder Cycloaddition. *Macromol. Chem. Phys.* **2017**, *218*, 1700050. [CrossRef]
117. Stieger, C.E.; Mcmillan, A.J.; de Geus, M.A.R.; Arafiles, J.V.V.; Franz, L.; Hackenberger, C.P.R. Unsaturated Phosphine Oxides for Modular Antibody Rebridging and Single Reagent Peptide-Cyclization-Bioconjugation. *Angew. Chem. Int. Ed.* **2025**, *64*, e202508656. [CrossRef]

Disclaimer/Publisher's Note: The statements, opinions and data contained in all publications are solely those of the individual author(s) and contributor(s) and not of MDPI and/or the editor(s). MDPI and/or the editor(s) disclaim responsibility for any injury to people or property resulting from any ideas, methods, instructions or products referred to in the content.